Table III. Angular Distribution of Scattered Light

θ, deg	P(θ)-(exptl)	P(θ)-(calcd)[a]	θ, deg	P(θ)-(exptl)	P(θ)-(calcd)[a]
30	0.455	0.456	105	0.083	0.082
37.5	0.357	0.355	120	0.070	0.069
45	0.278	0.278	135	0.063	0.061
60	0.186	0.185	142.5	0.058	0.057
75	0.131	0.131	150	0.057	0.056
90	0.102	0.102			

[a] Coils, $(\bar{F}^2)^{1/2} = 475$ nm.

but the extrapolated value of $C_{C\to 0}/I_{\theta\to 0}$ and extrapolated angular distribution of the light scattered are not modified. So, we can consider that the extrapolated values used for calculations are significant. The angular distribution of the light scattered fits with coil-shaped particles ($(\bar{F}^2)^{1/2} = 475$ nm) (Table III), in good agreement with the Brownian motion results. The molecular weight of the nonassociated species can also be calculated from the ultracentrifugation data, with use of the relationship available for flexible linear particles[39]

$$M = \left(\frac{\eta N}{\Phi^{1/3} P^{-1}}\right)^{3/2} \frac{s_0^{3/2}[\eta]^{1/2}}{10(1 - \bar{V}\rho)^{3/2}}$$

where η = solvent viscosity, N = Avogadro's constant, s_0 = sedimentation velocity for infinite dilution, $[\eta]$ = intrinsic viscosity of the solute, $\bar{V}$ = specific volume of the solute, and ρ = density of the solvent. $\Phi^{1/3}P^{-1}$ is taken to be equal to 2.5×10^6. This term was originally evaluated for polymers that are homogeneous with regard to the molecular weight. Validity of this treatment was tested for many systems by Mandelkern.[40] The average molecular weight of the polymeric species is found to be equal to 2.35×10^6, a value close to that determined by light-scattering experiments. The increase of the apparent sedimentation velocity with increasing concentrations for high dilutions can be discussed in terms of equilibrium displacement. When the concentration increases, the polymerization equilibrium is shifted toward the polymeric species and the average molecular weight increases, leading to an enhanced sedimentation velocity. For high concentrations, the equilibrium is shifted toward the polymeric species and the sedimentation is governed by the hydrodynamic effect.

These conclusions showing that polyvanadic acid colloids are polydispersed coils do not agree with some previous studies considering that colloidal vanadium pentoxide particles were rod shaped.[5-7] Such a rod-shaped model was taken in order to interpret the hydrodynamic properties of colloidal solutions, but it already did not agree very well with streaming birefringence experiments and the Kerr effect, and the discrepancies were then attributed to the presence of "molecular species" in the solution.

Acknowledgment. The authors wish to thank R. Morineau for electrical conductivity measurements.

Registry No. Vanadic acid, 11140-69-5; decavanadic acid, 12273-60-8.

(39) L. Mandelkern and P. J. Flory, *J. Chem. Phys.*, **20**, 212 (1952).

(40) L. Mandelkern, W. R. Krigbaum, M. A. Scheraga, and P. J. Flory, *J. Chem. Phys.*, **20**, 1392 (1952).

(41) M. M. Iannuzzi, C. P. Kubiak, and P. H. Rieger, *J. Phys. Chem.*, **80**, 541 (1976).

Contribution from the Department of Chemistry, The University of Texas at Arlington, Arlington, Texas 76019, and the Central Research Institute for Chemistry, Hungarian Academy of Sciences, H-1515 Budapest, Hungary

Kinetics and Mechanism of the Oxygenation of Bis(dimethylglyoximato)cobalt(II) in Methanol

L. I. SIMÁNDI,*[1a,b] C. R. SAVAGE,[1b] Z. A. SCHELLY,*[1b] and S. NÉMETH[1c]

The oxygenation of bis(dimethylglyoximato)cobalt(II) (cobaloxime(II), Cox) has been studied by the stopped-flow technique. A new experimental method, based on the in situ preparation of the complex, has been developed to eliminate the necessity of anaerobic work. The oxygenation of cobaloxime(II) consists of three distinct stages: (1) formation of μ-peroxo-dicobaloxime(III), $Cox(O_2)Cox$, in a rapid process, followed by (2) its slower disproportionation to μ-superoxo-dicobaloxime(III), $Cox(O_2)Cox^+$, and stable cobaloxime(III) and (3) solvolytic decomposition of $Cox(O_2)Cox^+$ to cobaloxime(III). At $Hdmg^-$ to cobalt(II) ratios of 4:1 and higher, the μ-peroxo complex produces a transient maximum in the stopped-flow traces recorded at 440-465 nm. The spectral changes necessary for this are ascribed to the presence of a μ-peroxo species containing unidentate $Hdmg^-$ coordinated in its two axial positions. The kinetics of the individual stages have been studied, and their mechanisms are discussed. Numerical values of the rate and equilibrium constants involved are reported.

Introduction

Bis(dimethylglyoximato)cobalt(II), $Co(Hdmg)_2$, often referred to as cobaloxime(II), has been extensively studied as a vitamin B_{12} model compound.[2-5] Cobaloxime(II) derivatives have been found to react with organic halides,[4-6] molecular hydrogen,[7-11] and dioxygen,[12] which makes them potentially important homogeneous catalysts. The activation of H_2 has been investigated in detail,[10,11] and some systems showing catalytic behavior have been reported,[10,13-15] although the

(1) (a) On leave of absence from the Central Research Institute for Chemistry, Hungarian Academy of Sciences, Budapest. (b) The University of Texas at Arlington. (c) Central Research Institute for Chemistry.
(2) Schrauzer, G. N. *Acc. Chem. Res.* **1968**, *1*, 97-103.
(3) Schrauzer, G. N. *Angew. Chem.* **1976**, *88*, 465-475.
(4) Schrauzer, G. N. *Pure Appl. Chem.* **1973**, *33*, 545-565.
(5) Pratt, J. M.; Craig, P. J. *Adv. Organomet. Chem.* **1973**, *11*, 331-446.
(6) Schneider, P. W.; Phelan, P. F.; Halpern, J. *J. Am. Chem. Soc.* **1969**, *91*, 77-81.
(7) Schrauzer, G. N.; Windgassen, R. J.; Kohnle, *Chem. Ber.* **1965**, *98*, 3324-3333.
(8) Simándi, L. I.; Szeverényi, Z.; Budo-Zâhonyi, E. *Inorg. Nucl. Chem. Lett.* **1975**, *11*, 773-777.
(9) Simándi, L. I.; Szeverényi, Z.; Budo-Zâhonyi, E. *Inorg. Nucl. Chem. Lett.* **1976**, *12*, 237-241.
(10) Simándi, L. I.; Budo-Zâhonyi, E.; Szeverényi, Z.; Németh, S. *J. Chem. Soc., Dalton Trans.* **1980**, 276-283.
(11) Chao, T. H.; Espenson, J. H. *J. Am. Chem. Soc.* **1978**, *100*, 129-133.
(12) Schrauzer, G. N.; Lee, L. P. *J. Am. Chem. Soc.* **1970**, *92*, 1551-1557.
(13) Ohgo, Y.; Takeuchi, S.; Yoshimura, J. *Bull. Chem. Soc. Jpn.* **1971**, *44*, 283-285, 583.

0020-1669/82/1321-2765$01.25/0

catalytic properties of these compounds are far from being fully utilized or understood. It was found that the cobaloxime(II) derivatives $BCo(Hdmg)_2$, where B is triphenylphosphine or pyridine, are active catalysts for the oxidation of hydroquinone, triphenylphosphine, and hydrazobenzene by dioxygen at atmospheric pressure and room temperature in benzene, acetone, or methanol.[16] In view of this fact, it is important to gain mechanistic information on the oxygenation of cobaloxime(II) derivatives, which is a key reaction in catalytic oxidations. In this paper a stopped-flow kinetic study is reported on the oxygenation of cobaloxime(II) in methanol.

Experimental Section

Cobalt(II) perchlorate (MCB) and dimethylglyoxime (Mallinckrodt) were reagent grade chemicals. Methanol was an MCB reagent containing 0.03% water. Nitrogen (99.999%) and oxygen (99.996%) were obtained from Air Products.

The stopped-flow spectrophotometer has been described earlier.[17] The reservoirs containing the reactant solutions were flushed with the gas required by the given experiment (N_2, O_2, or air). The gases were saturated with methanol before entering the system. In a typical experiment, one reservoir contained a solution of cobalt(II) perchlorate in methanol, and the other one was filled with a solution of K(Hdmg), prepared from methanolic KOH and H_2dmg. A stream of the desired gas was passed through the reservoirs during the experiment. A gas lock was used to maintain a slight overpressure in the reservoirs. Special gastight reagent syringes were employed to prevent air from leaking into the reagent solutions. The stopped-flow traces were displayed on a Tektronix 5441 storage oscilloscope and photographed with a C-5B camera.

Visible spectra were recorded on a Cary 219 instrument.

Results and Discussion

The air sensitivity of cobaloxime(II) derivatives, especially in solution, requires careful anaerobic work when these compounds are handled. There is an immediate change in color when a cobaloxime(II) solution prepared under an inert gas is exposed to air, indicating that oxygenation and/or oxidation is fast and requires the stopped-flow technique for kinetic investigations, as has been the case with some cobalt(II) polyamine complexes.[18-20] In a manner similar to these studies, in principle, O_2-saturated methanol can be mixed in the stopped-flow apparatus with a cobaloxime(II) solution prepared under an inert gas and the ensuing reaction can be monitored spectrophotometrically. There is, however, another possible approach, based on the known rapidity of cobalt(II) complex formation. If the formation of $Co(Hdmg)_2$ from Co^{2+} and $Hdmg^-$ ions is faster than the subsequent reaction of $Co(Hdmg)_2$ with dioxygen, then no anaerobic work is required, because the cobaloxime(II) solution can be prepared in situ. Air- or dioxygen-saturated solutions of cobalt(II) perchlorate and $Hdmg^-$ can be mixed in a stopped-flow device to form $Co(Hdmg)_2$, which will then react with O_2, with the spectrophotometric trace referring to the oxygenation process.

In order to test this hypothesis, we have compared the stopped-flow traces observed upon mixing methanol solutions of cobalt(II) perchlorate and $Hdmg^-$ under the following conditions: (1) both solutions purged from O_2 by a stream of high-purity N_2; (2) both solutions saturated with O_2. The traces obtained differ considerably. When the solutions are purged with N_2 for 3 h, there is barely any reaction discernible as indicated by the practically constant absorbance level after the flow stops (a slight change during the first 100 ms is due to residual O_2 impurity). On the other hand, a marked change in absorbance can be observed when O_2-saturated solutions are mixed. This implies that the formation of $Co(Hdmg)_2$ is complete within the time of mixing, indicating that the oxygenation of cobaloxime(II) can be conveniently followed by mixing O_2-saturated solutions of metal ion and ligand.

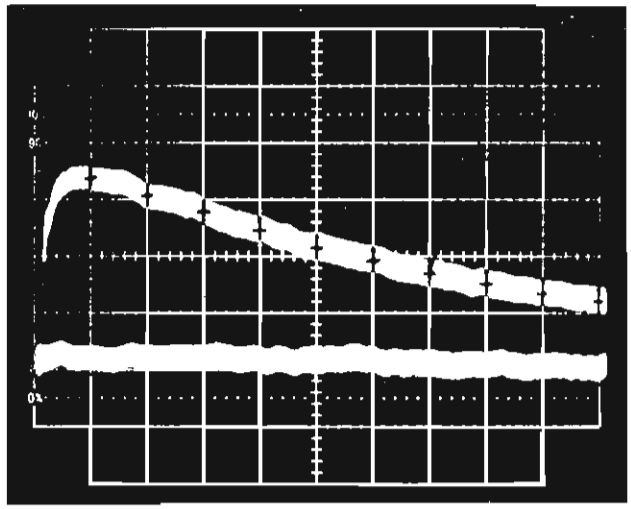

Figure 1. Accumulation and decay of the intermediate observed at 446 nm, with $[Co(ClO_4)_2]_0 = 1.5 \times 10^{-4}$ M, $[Hdmg^-]_0 = 1.32 \times 10^{-3}$ M, $T = 20$ °C, and solutions saturated with O_2. The time scale is 1 s/division, and the vertical scale is ~0.625(% T)/division.

Intermediates. In protic solvents such as methanol or water, cobaloxime(II) derivatives are irreversibly oxidized by dioxygen, resulting in the formation of cobaloxime(III) complexes, a fact widely utilized in synthetic procedures aimed at preparing bis(dimethylglyoximato)cobalt(III) compounds. The overall stoichiometry for the oxidation of $Co(Hdmg)_2$ is

$$4Co(Hdmg)_2 + O_2 + 2H_2O \rightarrow 4Co(Hdmg)_2O \quad (1)$$

which must apparently be a multistep process. In order to determine whether any intermediate(s) can be detected by the stopped-flow technique, we have monitored the reaction at various wavelengths in the 400–500-nm range, where cobaloxime(II) has a characteristic band.[10] The search for intermediates and the investigation of the trace forms have revealed the following facts.

(1) The accumulation and decay of a short-lived intermediate can be observed on traces recorded at 440–470 nm, at $Hdmg^-$ to cobalt(II) ratios equal to or larger than 4:1 (Figure 1).

(2) No intermediate can be detected if the $Hdmg^-$ to cobalt(II) ratio has the stoichiometric value of 2:1.

(3) As a consequence of the above, the trace at 470 nm depends on the ligand to metal ratio; at the stoichiometric value of 2:1, the absorbance increases with time, whereas at an 8.8-fold excess of $Hdmg^-$, the absorbance decreases with time, after having rapidly reached a maximum in about 100 ms.

(4) All traces consist of three distinct sections, even if no intermediate appears under the given conditions. The first and fastest phase of the reaction is over in about 100 ms, being followed by two slower processes, which extend to about 5–10 s and about 1–3 min, respectively (Figure 2).

Using the stopped-flow traces recorded between 400 and 500 nm, we have determined the absorbance values corresponding to times $t = 0$ (time when the flow stops), $t = 100$ ms, $t = 10$ s, and $t = 120$ s (end of reaction; this spectrum was also recorded on the Cary 219 spectrophotometer). The spectra emerging from these data are shown in Figures 3 and 4 for two different ligand to metal ratios. The initial spectra in both figures are closely similar to the known spectrum of

(14) Ricroch, M. N.; Gaudemer, A. *J. organomet. Chem.* **1974**, *67*, 119–129.
(15) Yamaguchi, T.; Miyagawa, R. *Chem. Lett.* **1978**, 89–92.
(16) Németh, S.; Szeverényi, Z.; Simándi, L. I. *Inorg. Chim. Acta* **1980**, *44*, L107–109.
(17) Wong, M. M.; Schelly, Z. A. *Rev. Sci. Instrum.* **1973**, *44*, 1226–1230.
(18) Simplicio, J.; Wilkins, R. G. *J. Am. Chem. Soc.* **1969**, *91*, 1325–1329.
(19) Miller, F.; Simplicio, J.; Wilkins, R. G. *J. Am. Chem. Soc.* **1969**, *91*, 1962–1967.
(20) Miller, F.; Wilkins, R. G. *J. Am. Chem. Soc.* **1970**, *92*, 2687–2691.

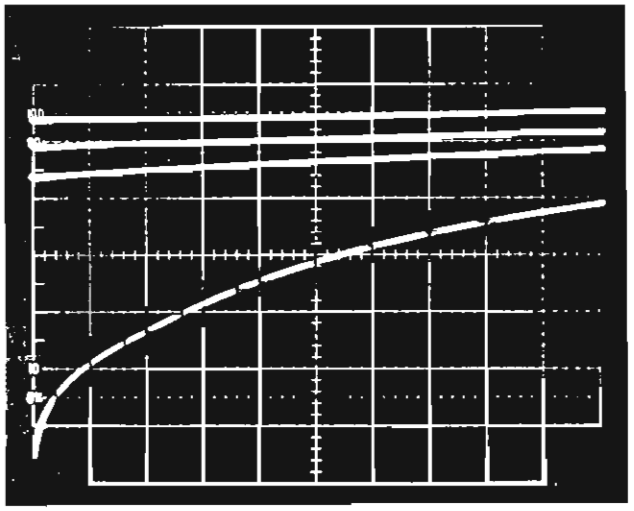

Figure 2. Stopped-flow trace taken at 400 nm illustrating the three distinct phases of the reaction, with $[Co(ClO_4)_2]_0 = 1.5 \times 10^{-4}$ M and $[Hdmg^-]_0 = 3.0 \times 10^{-4}$ M. The time scale is 1 s/division, and the vertical scale is −6.25(% T)/division. Phase 1 ends at about 0.2 s, phase 2 is over at about 10 s, and phase 3 is observed upon repeated triggering (upper three traces with decreasing slopes).

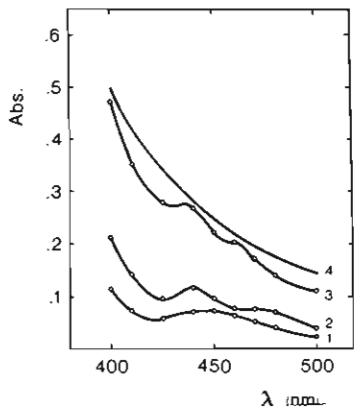

Figure 3. Time evolution of the absorption spectrum of the reaction mixture constructed from stopped-flow traces recorded at various wavelengths, at stoichiometric metal to ligand ratio, with $[Co(ClO_4)_2]_0 = 1.5 \times 10^{-4}$ M, $[Hdmg^-]_0 = 3.0 \times 10^{-4}$ M, and solutions saturated with O_2: (1) time $t = 0$; (2) $t = 100$ ms after mixing; (3) $t = 10$ s after mixing; (4) $t = 3$ min after mixing (Cary 219).

$Co(Hdmg)_2$ in methanol.[10] However, the apparent molar absorptivities are markedly lower than the values known from previous work. This indicates that already at $t = 0$, the solution contains at least one additional cobaloxime species that absorbs less strongly than $Co(Hdmg)_2$. The spectra obtained after the completion of the reaction are clearly of the cobaloxime(III) type and agree with the spectra of air-oxidized solutions. The two spectra in Figure 3 constructed from the absorbances at $t = 100$ ms and $t = 10$ s are those of an intermediate, superimposed on increasing amounts of the cobaloxime(III) product. Direct kinetic detection is not possible at this composition (ligand to metal ratio 2:1) since the absorbance increases monotonically in going from reactants to products, but the presence of an intermediate is indicated by the two bands in the transient spectra. However, direct kinetic observation of the intermediate becomes possible at $Hdmg^-$ to cobalt(II) ratios greater than 4:1 (Figures 1 and 4). Apparently, excess $Hdmg^-$ changes the spectrum of the intermediate so that a transient maximum in the absorbance appears at a given wavelength (e.g., at 446 nm). It should be noted that excess KOH does not produce a transient maximum. We checked this possibility because the $Hdmg^-$ solutions were prepared by

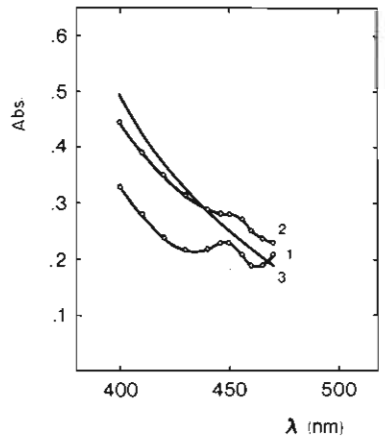

Figure 4. Time evolution of the absorption spectrum of the reaction mixture constructed from stopped-flow traces recorded in the presence of excess $Hdmg^-$, with $[Co(ClO_4)_2]_0 = 1.5 \times 10^{-4}$ M, $[Hdmg^-]_0 = 1.32 \times 10^{-3}$ M, and solutions saturated with O_2: (1) time $t = 0$; (2) $t = 100$ ms after mixing; (3) $t = 3$ min after mixing (Cary 219).

mixing equivalent amounts of KOH and H_2dmg. As to the question of why excess $Hdmg^-$ produces a transient maximum in the kinetic traces, we propose that it is due to the formation of a species where $Hdmg^-$ occupies the axial positions of the μ-peroxo-dicobaloxime(III) intermediate, whose structure will be discussed later in this paper.

Kinetic Measurement. The stopped-flow experiments with in situ cobaloxime(II) preparation were carried out at 400 and 470 nm, where conveniently large and characteristic absorbance changes are observed. The solubility of O_2 in methanol imposes certain limitations on the cobaloxime(II) concentrations used. So that an excess of dioxygen can be ensured, the maximum permissible cobaloxime(II) concentration should not exceed about 40% of the O_2 concentration, with allowance for an O_2 consumption of not more than 10%. The lower limit of cobaloxime(II) concentration is determined by the sensitivity of the stopped-flow spectrophotometer and the signal to noise ratio. The minimum absorbance change measurable with our instrument is 0.01, which was found to be the case in reactions with cobaloxime(II) concentrations of 5×10^{-5} M or higher.

The fact that the stopped-flow traces consist of three *distinctly* different sections permits us to treat each phase separately. The fast initial process is practically over in about 100 ms, which is roughly 1–2% of the estimated time needed for the second reaction to go to completion. Data for the fast section were obtained from suitably expanded traces, permitting accurate reading of A_∞.

We have found that the kinetic behavior of the fast initial process is consistent with a two-step mechanism (eq 2 and 3) describing the formation of μ-peroxo-dicobaloxime(III) from dioxygen and $Co(Hdmg)_2$, henceforth denoted by Cox.

$$Cox + O_2 \overset{K_1}{\rightleftharpoons} Cox(O_2) \qquad (2)$$

$$Cox(O_2) + Cox \underset{k_{32}}{\overset{k_{23}}{\rightleftharpoons}} Cox(O_2)Cox \qquad (3)$$

The μ-peroxo-dicobaloxime(III), $Cox(O_2)Cox$, was first isolated in the case of (pyridine)- and (triphenylphosphine)-cobaloxime(II) from CH_2Cl_2 solution by Schrauzer and Lee.[12] Similar dinuclear dioxygen complexes are abundantly encountered in the chemistry of cobalt(II) oxygen carriers.[21]

We assume that step 2 is a fast equilibrium with significant concentration of $Cox(O_2)$. This assumption is required by the initial spectrum, which shows contribution from an additional

(21) Jones, R. D.; Summerville, D. A.; Basolo, F. *Chem. Rev.* **1979**, *79*, 139–179.

Table I. Rate and Equilibrium Constants for Reactions 2 and 3 Based on the Fit of Eq 6 to the Stopped-Flow Traces of the Fast, Initial Phase[a]

$K_1 = 1400 \pm 150\ M^{-1}$	$k_{23} = (1.9 \pm 0.9) \times 10^6\ M^{-1}\ s^{-1}$
$K_{23} = (1.4 \pm 0.8) \times 10^5\ M^{-1}$	$k_{32} = 16 \pm 6\ s^{-1}$

[a] Error limits are standard deviations from the mean. Conditions: $T = 20$ °C; wavelength 400 nm; methanol solvent saturated with O_2 (solubility[22] of O_2 is 1.1×10^{-3} M) or air (O_2 concentration is 2.2×10^{-4} M); $[Co(ClO_4)_2]_0 = (0.5\text{–}1.5) \times 10^{-4}$ M; $[Hdmg^-]_0 = (1.0\text{–}3.0) \times 10^{-4}$ M.

cobaloxime species. The establishment of equilibrium 2 is too fast to be observed by the stopped-flow apparatus. The first, fast observable process corresponds to step 3, in which the components of equilibrium 2 are coverted to μ-peroxo-dicobaloxime(III).

Let us define $[Cox]_T$ as

$$[Cox]_T = [Cox] + [Cox(O_2)] = [Cox]_0 - 2[Cox(O_2)Cox] \quad (4)$$

i.e., the sum of the instantaneous concentrations of species in rapid equilibrium with each other. The rate of formation of $Cox(O_2)Cox$ is

$$\frac{d[Cox(O_2)Cox]}{dt} = k_{23}[Cox(O_2)][Cox] - k_{32}[Cox(O_2)Cox] \quad (5)$$

Rate equation 5 can be written in terms of $[Cox]_T$ as the independent variable, which after integration yields

$$\ln \frac{([Cox]_0 - [Cox]_{T,\infty})(1 + D[Cox]_T)}{([Cox]_T - [Cox]_{T,\infty})(1 + D[Cox]_0)} = k_{obsd}t \quad (6)$$

where

$$D = \frac{[Cox]_0 - [Cox]_{T,\infty}}{[Cox]_0[Cox]_{T,\infty}} \quad (7)$$

and

$$k_{obsd} = \frac{2K_1k_{23}[O_2]}{(1 + K_1[O_2])^2} \frac{[Cox]_{T,\infty}(2[Cox]_0 - [Cox]_{T,\infty})}{[Cox]_0 - [Cox]_{T,\infty}} \quad (8)$$

and the subscript ∞ refers to equilibrium. Due to the low cobaloxime(II) concentrations used, the concentration of dissolved oxygen is assumed to be constant[22] during the reaction.

The fast first sections of the stopped-flow traces were found to yield first-order plots with a reproducible curvature. This implies that the factor $(1 + D[Cox]_T)/(1 + D[Cox]_0)$ in eq 6 deviates from unity, indicating non-first-order behavior. In order to determine the rate and equilibrium constants involved, we have fitted eq 6 to the experimental curves, using a steepest descent type program combined with a simplex search. The problem was set up in terms of four parameters. The results of the optimization are listed in Table I. A key step in determining rate constant k_{23} is the estimation of K_1 from the ratio of the k_0 values for solutions saturated with dioxygen and air. This calculation gave $K_1 = 1400 \pm 150\ M^{-1}$, which was used to determine k_{23} from the best fit k_0 value for each run. The overall equilibrium constant K_1k_{23} was calculated from the best fit value of $[Cox]_{T,\infty}$. The known K_1 permits us to obtain k_{23} from this product, which in turn yields k_{32}. Figure 5 illustrates the agreement between experimental and calculated traces.

Kinetic measurements performed with air- and dioxygen-saturated solutions have yielded consistent rate and equilibrium

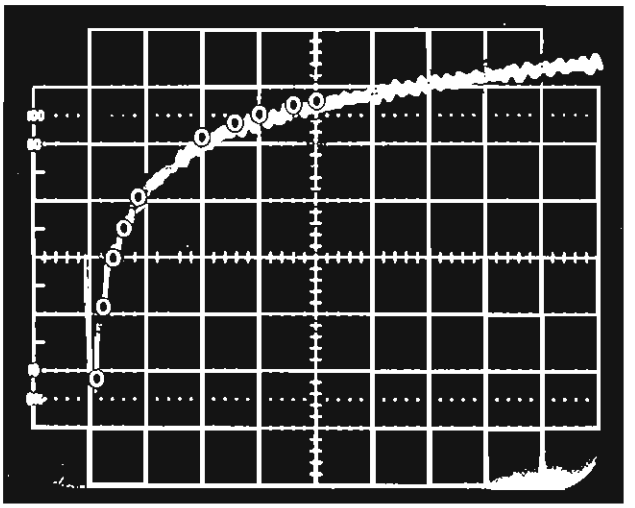

Figure 5. Typical stopped-flow trace of the fast, initial phase with points indicating values calculated by using the best fit parameters. The agreement is within the experimental error up to about 80 ms, where the second phase starts to become noticeable; $[Co(ClO_4)_2]_0 = 1.5 \times 10^{-4}$ M and $[Hdmg^-]_0 = 3.0 \times 10^{-4}$ M, with methanol solvent saturated with O_2. The time scale is 20 ms/division, and the vertical scale is $-2.5(\%\ T)$/division.

constants, indicating that the first fast phase of the reaction is indeed the two-step oxygenation of $Co(Hdmg)_2$. In experiments with air-saturated solutions, the O_2 concentration was taken equal to 2.2×10^{-4} M, which is one-fifth of the solubility of O_2 in methanol when saturated with pure dioxygen.

Since the short-lived intermediate detected reaches its maximum concentration at times corresponding to the end of the fast phase, it is reasonable to assume that the intermediate is the μ-peroxo-dicobaloxime(III), $Cox(O_2)Cox$. In the presence of excess $Hdmg^-$, its spectrum is changed (cf. Figures 5 and 6) relative to that observed for the stoichiometric composition. We propose that this is due to the axial coordination of $Hdmg^-$ as a unidentate ligand via its oximato group, resulting in structure I. To our knowledge, this type of $Hdmg^-$

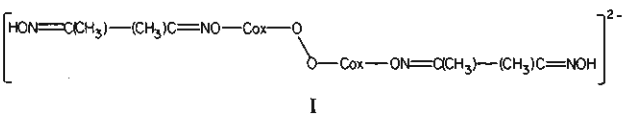

I

coordination has not been postulated thus far. The suggestion is based on the fact that the starting spectra (at $t = 0$) are different in the presence and absence of excess $Hdmg^-$ (Figures 3 and 4) under O_2 atmosphere. As we have detected no difference between the spectra (with and without excess $Hdmg^-$) when recorded *under Ar*, we conclude that axial bonding takes place in $Cox(O_2)$ and possibly $Cox(O_2)Cox$ and is much faster than expected for most cobalt(III) complexes.[23] This is in line with earlier reports on fast ligand exchange in cobaloxime(III) derivatives, especially if catalytic amounts of cobaloxime(II) are present.[24,25]

Analysis of the second, slower section of the traces has shown that good second-order plots ($1/(A_\infty - A)$ vs. time) can be obtained up to 6–10 s, which corresponds to the end of this phase. Since O_2 is directly involved in the fast initial section only, the second phase can be studied also at higher cobal-

(22) The solubility of O_2 in methanol is 1.1×10^{-3} M at 20 °C (Kretschmer, C. B.; Nowakowska, J.; Wiebe, R. *Ind. Eng. Chem.* **1946**, *38*, 506–509).

(23) Basolo, F.; Pearson, R. G. "Mechanisms of Inorganic Reactions"; Wiley: New York, 1967.

(24) Marzilli, L. G.; Salerno, J. G.; Epps, L. A. *Inorg. Chem.* **1972**, *11*, 2050–2053.

(25) Courtright, R. L.; Drago, R. S.; Nusz, J. A.; Nozari, M. S. *Inorg. Chem.* **1973**, *12*, 2809–2815.

Table II. Apparent Second-Order Rate Constant (k_2) for the Disproportionation of μ-Peroxo-dicobaloxime(III) (Second, Slower Section, Eq 10)[a]

$10^4 \times [Co(ClO_4)_2]_0$, M	$10^4 \times [Hdmg^-]_0$, M	$10^{-4}k_2$, M^{-1} s^{-1}
0.50	1.00	2.38
0.50	1.00	2.19
0.50	1.00	2.03
0.50	1.00	1.88[b]
0.50	1.00	2.21[b]
0.50	1.00	2.30[b]
0.50	1.10	1.27
0.50	1.10	1.22
1.50	6.60	2.58
1.50	6.60	2.30
1.50	13.20	0.17
1.50	13.20	0.21
1.50	13.20	0.19

[a] Conditions: $T = 20$ °C, methanol solvent saturated with O_2, wavelength 470 nm. [b] Wavelength 400 nm.

oxime(II) concentrations, exceeding the limit set by the requirement of excess dioxygen. The slopes of the straight-line plots obtained from the kinetic traces recorded at 400 and 470 nm were converted to second-order rate constants (k_2, Table II), by estimating the difference between molar absorptivities from the intercept. Since $\Delta\epsilon$ refers to two short-lived intermediates, there is no other way of determining its value.

The second-order behavior of this phase is consistent with the observation of Schrauzer and Lee[12] that $Cox(O_2)Cox$ is converted to an ESR-active μ-superoxo-dicobaloxime(III), $Cox(O_2)Cox^+$, via a disproportionation process. In methanol as solvent, the stoichiometry of this reaction is

$$4Cox(O_2)Cox + 3H_2O \rightarrow 2Cox(O_2)Cox^+ + 4Cox(OH) + {}^1/_2O_2 + 2OH^- \quad (9)$$

where Cox(OH) denotes hydroxocobaloxime(III). One of the axial positions in all cobaloxime(III) species is occupied by a solvent molecule. The solvent methanol used in this work contained enough water (about 2×10^{-2} M) necessary for (9). It was not investigated whether MeOH instead of H_2O participates in eq 9 since our main concern was the nature of the redox processes directly involving the various cobaloxime species.

The mechanism of disproportionation 9 can be written as a water- or solvent-assisted rate-determining step:

$$2Cox(O_2)Cox \xrightarrow[1.5H_2O]{k_2} Cox(O_2)Cox^+ + 2Cox(OH) + {}^1/_4O_2 + OH^- \quad (10)$$

The rate constant k_2 in Table II decreases with increasing excess of $Hdmg^-$ over cobalt(II) in the initial reactant mixture, which indicates a lower reactivity of the six-coordinate μ-peroxo-dicobaloxime(III) I in the disproportionation step (10). This is in line with the electrostatic repulsion between the two species I in the rate-determining step (10).

The slowest, third section of the stopped-flow traces extending up to 60 s and beyond was found to obey first-order kinetics, yielding linear plots of log $(A_\infty - A)$ vs. time. The first-order rate constants k_3 for this phase are listed in Table III. It is independent of the wavelength of observation and the ligand to metal ratio, as well as of the O_2 concentration in the solution. We assign this reaction to the decomposition of μ-superoxo-dicobaloxime(III) to stable cobaloxime(III) complexes and dioxygen. The sensitivity of $Cox(O_2)Cox^+$ to nucleophilic attack has been noted before.[12] This is in agreement with the rapid decomposition in the strongly nucleophilic medium used in the present work. We propose a mechanism for this reaction in which the rate-determining step is the first-order hydrolysis (or solvolysis)

$$Cox(O_2)Cox^+ + H_2O \xrightarrow{k_3} Cox\text{–}O_2H^+ + Cox(OH) \quad (11)$$

followed by the decomposition step

$$Cox\text{–}O_2H^+ + Cox(O_2)Cox^+ + H_2O \xrightarrow{\text{fast}} Cox(OH) + 2Cox^+ + 1.5O_2 \quad (12)$$

(Cox^+ is a cobaloxime(III) species with solvent molecules in both axial positions; it may eventually be converted to Cox(OH) or Cox(OMe).)

The species $Cox\text{–}O_2H^+$ in eq 11 is a mononuclear superoxocobaloxime(III), whose deprotonated form has been reported to exhibit an eight-line ESR spectrum in CH_2Cl_2.[12] It does not appear to be stable in methanol under the conditions used in this work.

Equations 11 and 12 can also be written in terms of cobaloxime(III) species derived from I as the precursor of $Cox(O_2)Cox^+$. Axially coordinated $Hdmg^-$ does not influence the rate of step 11 as evidenced by the data in Table III.

Table III. First-Order Rate Constants (k_3) for the Solvolytic Decomposition of μ-Superoxo-dicobaloxime(III) (Third, Slowest Section, Eq 11)[a]

$10^4 \times [Co(ClO_4)_2]_0$, M	$10^4 \times [Hdmg^-]_0$, M	wavelength, nm	10^2k_3, s^{-1}
1.5	3.0	400	3.22
0.5	1.0	400	3.86
0.5	1.1	400	4.02[b]
0.5	1.1	400	3.90[b]
1.5	3.3	470	3.10[b]
1.5	13.2	470	3.27
1.5	13.2	470	3.56
			av 3.56 ± 0.37

[a] Conditions: $T = 20$ °C, methanol solvent saturated with O_2. [b] Solutions saturated with air.

The results reported in this work provide independent kinetic support for the oxygenation scheme proposed by Schrauzer and Lee[12] on the basis of the identification of the ESR-active $Cox(O_2)Cox^+$ and $Cox\text{–}O_2$ species. The mechanisms proposed for the individual phases of the overall reaction take into account the effect of the protic solvent used and rationalize the apparently complex stoichiometries.

Acknowledgment. L.I.S. thanks the Department of Chemistry, UTA, for a Visiting Professorship during the summer of 1980. Financial support by the Robert A. Welch Foundation is gratefully acknowledged.

Registry No. Cox, 36451-49-7.